

1
2
3
4
5
6
7
8
9
10
11
12
13
14
15
16
17
18
19
20
21
22
23
24
25
26
27
28
29
30
31
32

Received data: : 03-Jun-2015

Accept Date: 29-Sep-2015

Article Type: Standard Paper

Editor :Roberto Salguero-Gómez

Corresponding author email-id: cmetcalf@princeton.edu

Opportunities and challenges of Integral Projection Models for modelling host-parasite dynamics

A manuscript in consideration as a research paper for publication in Journal of Animal Ecology as part of the Special Feature *Demography beyond the Population*.

C.J.E. Metcalf^{1,2}, A.L. Graham¹, Martinez-Bakker, M.³, D.Z. Childs⁴

¹Department of Ecology and Evolutionary Biology, Princeton University, Princeton, USA

²Office of Population Research, the Woodrow Wilson School, Princeton University, Princeton, USA

³Department of Ecology and Evolutionary Biology, University of Michigan, USA

⁴Department of Animal and Plant Sciences, Sheffield University, Sheffield, UK

keywords: Integral Projection Model, parasite, demography, infectious disease, dynamics, murine malaria, measles

This is the author manuscript accepted for publication and has undergone full peer review but has not been through the copyediting, typesetting, pagination and proofreading process, which may lead to differences between this version and the [Version of Record](#). Please cite this article as [doi: 10.1111/1365-2656.12456](https://doi.org/10.1111/1365-2656.12456)

This article is protected by copyright. All rights reserved

33

34 **Summary**

- 35 1. Epidemiological dynamics are shaped by and may in turn shape host
36 demography. These feedbacks can result in hard to predict patterns of disease
37 incidence. Mathematical models that integrate infection and demography are
38 consequently a key tool for informing expectations for disease burden, and
39 identifying effective measures for control.
- 40 2. A major challenge is capturing the details of infection within individuals and
41 quantifying their downstream impacts to understand population scale
42 outcomes. For example, parasite loads and antibody titers may vary over the
43 course of an infection, and contribute to differences in transmission at the
44 scale of the population. To date, to capture these subtleties, models have
45 mostly relied on complex mechanistic frameworks, discrete categorization,
46 and/or agent based approaches.
- 47 3. Integral Projection Models (IPMs) allow variance in individual trajectories of
48 quantitative traits and their population level outcomes to be captured in ways
49 that directly reflect statistical models of trait-fate relationships. Given
50 increasing data availability, and advances in modeling, there is considerable
51 potential for extending this framework to traits of relevance for infectious
52 disease dynamics.
- 53 4. Here, we provide an overview of host and parasite natural history contexts
54 where IPMs could strengthen inference of population dynamics, with
55 examples of host species ranging from mice to sheep to humans, and parasites
56 ranging from viruses to worms. We discuss models of both parasite and host
57 traits, provide two case studies, and conclude by reviewing potential for both
58 ecological and evolutionary research.

59 **Introduction**

60 Over the course of an infection, as the parasite replicates and evades or overcomes the
61 host's defences, parasite density, size or abundance and associated immune responses
62 fluctuate, often following complex trajectories (Metcalf *et al.* 2011). These
63 fluctuations shape host and parasite population level outcomes via their effects on
64 rates of host recovery, pathology, between host transmission, and waning of host
65 immunity (Gilchrist, Coombs & Perelson 2004; Graham *et al.* 2007). Constructing
66 mechanistic models that capture the detail of these fluctuations is complicated by the

67 array of effectors associated with the immune response, the abundance of feedbacks
68 designed to keep potentially harmful immune responses in check (Graham, Allen &
69 Read 2005), the complex role of host memory (Antia, Ganusov & Ahmed 2005), and
70 the dynamic nature of parasite growth itself (Antia & Lipstich 1997). Examples of
71 analytical models (generally built around Partial Differential Equations) based on
72 empirical data include models developed for HIV (Perelson 2002), influenza (Saenz *et*
73 *al.* 2010) and malaria in murine (Haydon *et al.* 2003; Mideo *et al.* 2008) and human
74 hosts (Molineaux & Dietz 1999). For these examples, considerable data and detailed
75 biological knowledge are available, and models have further deepened our
76 understanding of the processes driving the time course of infection. Nevertheless,
77 model development and appropriate parameterization in the face of available data
78 remains non-trivial (non-linear feedbacks result in extremely erratic likelihood
79 surfaces, leading to ambiguity in parameter estimates); and further, efforts to extend
80 these models to connect within-host dynamics to population outcomes remain rare
81 (Gog *et al.* 2014).

82 Linking individuals to population outcomes is of fundamental relevance for
83 both ecological and evolutionary questions (Metcalf *et al.* 2014). Population scale
84 questions such as the impact of coinfection on transmission (Graham *et al.* 2007), the
85 spread of resistance mutations in the face of chemotherapy (Kouyos *et al.* 2014), or
86 determinants of spillover, in terms of what makes populations viable reservoirs
87 (Brook & Dobson 2015) require cross scale models capable of capturing individual
88 differences, and integrating across them to evaluate population level outcomes.

89 Many of the variables that drive the key processes linking individuals to
90 populations (transmission potential, host survival, etc.) have in common the fact that
91 they are quantitative traits (for example, concentrations of virions, unicellular
92 parasites, antibodies and lymphocytes in the blood). Integral Projection Models
93 (IPMs) are now broadly used in ecology and evolution to capture demographic
94 outcomes linked to continuous individual level variables such as size (Easterling,
95 Ellner & Dixon 2000; Childs *et al.* 2011; Merow *et al.* 2014). Focal variables
96 generally reflect individual life history or physiological traits such as size, weight,
97 height, snout to vent length, tarsus length, etc. The dynamics of these traits (for
98 example, increases in size via growth, or losses via shrinkage) and their links to
99 survival or fertility, are modelled using generalized linear regression approaches
100 (Easterling, Ellner & Dixon 2000). A transition kernel reflecting these functions

101 defines transitions between sizes (or other chosen traits) over a discrete time-step,
102 usually a year. In the simplest analysis, the structure of the transition kernel is
103 broadly analogous to a classic matrix population model (Caswell 2001) with a
104 diagonal reflecting transitions linked to growth and survival, and another important
105 transition area linking adult size to offspring size. The key difference is that rather
106 than discrete probabilities describing how individuals in a particular stage might be
107 distributed across the range of possible stages at the next time step, a density relates
108 current size to the continuous distribution of future sizes.

109 One of the major strengths of the IPM approach is that their formulation via a
110 probability density allows inclusion of variation in trajectories across individuals and
111 through time. For evolutionary models of continuous traits such as size at flowering of
112 monocarpic plants (Metcalf *et al.* 2008), or ecological models exploring the impact of
113 changes in body size on population dynamics (Ozgul *et al.* 2010), capturing these
114 details can be key. Selection on life histories, in particular, will be modified by
115 individual variation in trajectories – for example, the variance in growth trajectories of
116 individuals from the same genetic background decreases the optimal flowering size in
117 monocarpic plants (Childs *et al.* 2003), and including individual variation this is
118 therefore essential for inference.

119 In the context of infectious disease dynamics, an IPM framework can capture
120 consistent individual differences as well as temporal fluctuations in antibody titer,
121 other metrics of immunological activity, and their downstream effects on within-host
122 parasite abundance, which might result from varied nutritional status and/or history of
123 infection. Furthermore, and importantly, the impact of individual trajectories on
124 individual host level outcomes, such as survival, and resulting population level
125 characteristics, such as transmission, can be appropriately reflected. IPMs have been
126 deployed to explore transmission of fungal parasites across a size structured coral
127 population (Ellner *et al.* 2007); the impact of fungal symbionts on the population
128 growth rate of two grass species (Chung, Miller & Rudgers 2015), ant symbionts on
129 the population growth rate of a cactus (Ford *et al.* 2015), and a variant has been used
130 to explore heritability of set point viral loads (Bonhoeffer *et al.* 2015). All of these
131 have yielded insights into the process of transmission, or the effect of the pathogen on
132 population dynamics, but to date there has been relatively little work capitalizing on
133 the strengths of IPMs in the context of within-host dynamics and the population
134 ecology of infectious diseases in mammals.

135 Here, we start by introducing the broad categories of infectious-disease related
136 traits that might be modelled using an IPM approach, and the some of the questions
137 that could be tackled with such an approach; and then move on to examine two case
138 studies on murine malaria and maternal antibodies against measles; we conclude by
139 discussing when an IPM approach might be most appropriate, and key future
140 directions.

141

142 **IPMs for host-parasite dynamics**

143 Infectious disease dynamics inherently contain at least two species (the parasite and
144 the host) - and this number is increased where multi-host parasites, or spillover from
145 one host into another are the focus. Building on developments in modelling complex
146 life-cycles with IPMs (Ellner & Rees 2006; Metcalf *et al.* 2013) and modelling
147 infectious disease dynamics in structured populations (Klepac & Caswell 2011), it is
148 straightforward to adapt an IPM framework to efficiently capture traits of hosts,
149 parasites, or the combined host-parasite dyad.

150 Parasites can be broadly categorized into two groups – *acute parasites*,
151 associated with short duration infections; and *chronic parasites*, where infection is
152 long lasting. Often, this distinction aligns with the distinction between micro-parasites
153 (which multiply within the host) and macro-parasites (e.g., many helminths, which do
154 not). There are, of course, exceptions - microparasites such as HIV may result in
155 chronic infections. However, for both acute and chronic parasites, at the within host
156 scale, infection is an inherently dynamic process, reflected by changes in an array of
157 continuous traits.

158 To start with acute infections, parasite multiplication results in increasing
159 abundance and spread of the parasite within the host, but this is in turn mitigated by
160 both target cell depletion (where target cells are the resources targeted by the parasite)
161 and immune system activity (Graham 2008; Metcalf *et al.* 2011). As a result of these
162 interactions, a focal trait such as parasite load will tend to rapidly increase, and then
163 decrease. Capturing this in an IPM framework will typically require abstracting the
164 underlying dynamical details, as an IPM generally reflects broad features of trait
165 changes using regression tools (but see Discussion for possible extensions). One
166 option to appropriately capture the extreme changes observed over the course of an
167 acute infection is to include a further structuring of traits along an axis such as day
168 post infection (analogous to IPMs where individuals experience different transitions

169 across size for each age class (Childs *et al.* 2011), they can experience different
170 transitions across parasite load based on day post infection), illustrated below (Case
171 study 1). However, care will be required in estimating and interpreting the underlying
172 parameters, as many host-parasite IPMs will implicitly codify assumptions about host
173 and parasite traits and their relationship. For example, for an IPM describing the
174 dynamics of parasitemia, the parameter reflecting the initial parasite dose could
175 easily be increased to explore the effects on prevalence in the population. However,
176 results will be misleading if the model does not explicitly include what is likely to be
177 a non-linear relationship between initial parasite dose and the resulting host immune
178 response. Explicit codification could be achieved by defining a specific functional
179 form that links dose dependence and immune induction in the model, but if data are
180 not available with which to parameterize such a relationship (here, such data might
181 include multiple starting doses), then the assumed functional form is necessarily
182 speculative. This is, of course, a very general issue in model construction, but one
183 which may be of particular importance here, as the formulation of within host
184 dynamics (which are notoriously reactive) via regression tools may result in an array
185 of cryptic assumptions being made, and special care should be take to evaluating the
186 importance of these. As a result, the strongest inference may follow from
187 comparative analyses across different clones, pathogens, or hosts rather than
188 exploratory model perturbations and forward simulation – an example is provided in
189 the malaria model described below. Nevertheless, in some cases, of course,
190 interpretation of parameters linked to some aspects of host or parasite biology (e.g.,
191 host fertility, host mortality, parasite growth, and parasite reproduction) may be
192 straightforward and perturbation analyses may be a powerful direction for inference.

193 Parasite load is clearly not the only possible focal trait - for acute parasites,
194 infection will usually lead to a rapid increase in immune activation, including the rate
195 of proliferation of cells of the immune system, boosting of the signalling molecules
196 that the cells secrete, and production of antibodies specific to the parasite; all these
197 processes are often subsequently rapidly down-regulated to avoid immunopathology
198 (Graham, Allen & Read 2005). An array of related continuous features could be
199 modelled using an IPM-like framework. The scope for the potential array of models
200 here is enormous – the rate at which cells and molecules are induced and decay, and
201 the degree to which they provide indicators of exposure vs. disease may be both
202 parasite and effector specific. It is worth noting that some of the most successful

203 infectious disease models deployed to date have been powerful exactly because
204 immunity has such extreme dynamics that it effectively acts as a binary trait (i.e., for
205 completely immunizing infections such as measles, Bjørnstad, Finkenstadt & Grenfell
206 2002), allowing the detail of within host dynamics to be ignored. Nevertheless,
207 completely immunizing infections remain a relatively special case, and there is scope
208 for investigating immune dynamics related to an array of other parasites where, for
209 example, antibody titer provides a correlate of demographic outcomes, such as
210 mortality, or infection probability, relevant to bridging between scales. Even in the
211 case of immunizing infections, there are some areas where more subtle effects are
212 expected - maternal immunity provides a special case of antibody dynamics for
213 measles, discussed in detail below (Case study 2).

214 Moving to the case of chronic infections, for macro-parasites, such as
215 helminths, the parasites may grow within the host, increasing depletion of host
216 resources (Hayward *et al.* 2014b), but they do not generally increase in abundance
217 (apart from ingestion of additional transmission stages such as eggs). More generally,
218 for chronic parasites (which includes many macro-parasites), in mathematical terms,
219 we can often think of parasite density and the host's immune system (i.e., target cell
220 production) as settling to equilibrium. The details of the dynamics leading up to
221 equilibrium may be of less importance, and relative to acute infections it is thus more
222 straightforward to envisage capturing within host dynamics using regression tools, as
223 the extreme fluctuations in focal traits such as those that characterize acute infections
224 are avoided. Key continuous traits that might be modelled using an IPM framework
225 for chronic parasites might include parasite load (Bonhoeffer *et al.* 2015), the density
226 of parasite-specific lymphocytes (Borchers *et al.* 2014), or parasite length in the case
227 of helminths. Insights are likely to emerge from understanding either the trajectory to
228 the equilibrium (where this is amenable to regression modelling), but also and perhaps
229 more powerfully, the role of variance around the mean in parasite load, as was
230 explored in a recent paper by Bonhoeffer *et al.* (Bonhoeffer *et al.* 2015).

231 Approximating all populations and processes by Gaussian distributions, they derived
232 analytical expressions to describe change in the distribution of HIV set point load over
233 a single transmission cycle. In principle, their model could be reformulated as an IPM
234 to allow greater flexibility in the underlying distributional assumptions.

235 Chronic and acute pathogens will also elicit responses from the immune
236 system's enormously complex and frequently dynamic set of effectors. Some

237 components may be relatively constant, putting the emphasis for IPM based inference
238 more on capturing individual variance rather than capturing the details of the
239 trajectories through time. For example, titers of self-reactive antibody, a marker used
240 to identify auto-immune diseases, differ markedly among individuals, but are
241 consistent within individuals across time, thus providing a heterogeneous but static
242 individual trait (Vindenes & Langangen 2015), in contrast to the dynamic traits
243 described so far. In Soay sheep, self-reactive antibodies correlate positively with
244 survival and parasite-specific antibody, and negatively with annual fertility (Graham
245 *et al.* 2010). Parasite-specific antibodies provide additional power to predict survival
246 of individuals (Nussey *et al.* 2014). With detailed data available to translate such
247 variables into individual level consequences (for example, linking antibody titers to
248 host survival and fertility), an IPM approach could enable powerful exploration of the
249 population level consequences of trait heterogeneity across individuals, and the roles,
250 for example, of alternative modes of defence (such as resistance vs. tolerance) at the
251 epidemiological scale (Hayward *et al.* 2014a).

252 For both chronic and acute infections, successful construction of IPMs, or any
253 other models that bridge scales of biological processes, will require (i) modelling
254 within host dynamics (using regression tools in the case of IPMs), (ii) careful
255 interpretation of associated parameters, and (iii) robust translation of the chosen focal
256 trait into processes that have population level effects. Specifically, host traits such as
257 recovery, survival, or fertility (Figure 1) will translate to the population level of
258 disease dynamics, via their influence on transmission potential, which may also scale
259 with individual viral load or other features of within-host dynamics.

260

261 **Case study 1: estimating probability of onward transmission from within-host** 262 **dynamics of malaria**

263 In the bloodstream phase of malaria (*Plasmodium spp.*), infected red blood cells
264 (RBCs) burst in synchrony, releasing merozoites that may infect a new RBC. Twenty-
265 four or forty-eight hours later (depending on the malaria species) the next generation
266 of merozoites bursts out, and the cycle then repeats itself until the host dies or clears
267 the infection (Figure 2A). Over the course of the infection, a fraction of the infected
268 cells develop into sexual forms that are taken up by mosquitoes. When the mosquito
269 bites its next host, the parasite migrates to the liver. Parasites then emerge from the
270 liver, and the bloodstream phase starts again (Metcalf *et al.* 2012).

271 Here, to illustrate a population scale inference arising from IPM analysis of
 272 within-host dynamics, we leverage data describing the bloodstream phase of a range
 273 of clones of rodent malaria (*P. chabaudi*, described in Long *et al.* 2008a; Long *et al.*
 274 2008b; Metcalf *et al.* 2012) to explore the consequences of these within host
 275 dynamics for population level outcomes, specifically rates of onward transmission.
 276 We do so by nesting an IPM within a basic SIR population model. We model the
 277 within-host dynamics of this acute infection by tracking the log number of infected
 278 RBCs as our focal trait, denoted z . In principle, it is also possible to use the number of
 279 infected RBCs directly as the focal trait, leading to a matrix population model
 280 parameterized with regression tools. However, the log scale is more practical since the
 281 range of RBCs spans several orders of magnitude and never approaches zero. Infected
 282 RBC load shapes host survival, recovery, and transmission (Mackinnon & Read
 283 2004b); and thus is an appropriate focal trait. To also account for the dynamics of this
 284 acute 24h-cycling parasite over the course of the infection, we further structure our
 285 model by day post infection, ranging from 1 to J days post-infection. The form of the
 286 population model is:

$$\begin{aligned}
 S(t+1) &= sS(t)(1 - \phi_t) + fS(t) + f \sum_{j=1}^J \int_L^U I_j(z, t) dz + fR(t) \\
 I_0(z', t+1) &= s\phi_t S(t) G_0(z') dz \\
 I_{j+1}(z', t+1) &= \int_L^U G_j(z', z) s_z(z) (1 - r_j(z)) I_j(z, t) dz \quad [\text{for } j < (J - 1)] \\
 I_J(z', t+1) &= \int_L^U G_{J-1}(z', z) s_z(z) (1 - r_{J-1}(z)) I_{J-1}(z, t) dz + \int_L^U G_J(z', z) s_z(z) (1 - r_J(z)) I_J(z, t) dz \\
 R(t+1) &= \sum_{j=1}^J \int_L^U s_z(z) r_j(z) I_j(z, t) dz + sR(t)
 \end{aligned}$$

287
 288 where $S(t)$ indicates the number of susceptible individuals at time t , $I_j(z, t)$ captures the
 289 number of infected individuals at time t with log infected RBC load z , on day j post-
 290 infection (and the prime in $I_j(z', t+1)$ indicates that this reflects the log infected RBC
 291 load the following time-step), and $R(t)$ is the number of recovered individuals at time
 292 t ; U and L indicate the limits of integration across log infected RBC load, where the
 293 upper limit (U) reflects a value slightly larger than the maximum observed (which
 294 here reflects the maximum observed log infected RBC load); and likewise for the
 295 lower limit (L). Finally, J is the total number of days post infection modelled. Note

296 that the discrete time-unit for this compound IPM (compound because it is structured
 297 by both day post infection and log infected RBC load) is one day – it would also be
 298 possible to separate the time-scales of the within-host and between host dynamics
 299 (Heffernan & Keeling 2009), but we chose to keep them unified in the two case
 300 studies illustrated here. We model mouse fertility as a constant, captured by the
 301 parameter f , and survival as a constant captured by the parameter s , except in infected
 302 individuals whose survival is related to their parasite load z , as described by a
 303 probability $s_z(z)$. All of these parameters are adjusted to reflect one day to match the
 304 time-scale of the within-host infection process. The probability of infection is
 305 captured by ϕ_t , further described below. Upon infection, the distribution of log
 306 infected RBCs that hosts experience is captured by the density function $G_0(z)$;
 307 subsequent transitions between infected states is captured by the kernel $G_j(z',z)$; and
 308 the probability of recovery is described by $r_j(z)$; see Table 1 for details and functional
 309 forms.

310 The probability of infection of susceptible individuals, ϕ_t , must encompass the
 311 density of the asexual form (captured here by log infected RBCs, z), allocation by the
 312 asexual blood phase to the sexual form, ingestion of this form by a mosquito, and
 313 transmission to a new host. Although differences in allocation to sexual reproduction
 314 across clones and through time have been observed (Mackinnon & Read 1999; Long
 315 *et al.* 2008a; Long *et al.* 2008b; Metcalf *et al.* 2012), we initially ignore this
 316 complexity, and assume that uptake of the parasite by mosquitoes scales with the
 317 numbers of infected RBCs; modelling transmission as a frequency dependent process
 318 then captures vector borne transmission. Assembling these elements, the probability
 319 of infection of a susceptible individual is defined by:

$$320 \quad \phi_t = 1 - \exp\left(-\beta \sum_{j=1}^J \int_L^U I_j(z, t) z / N_t dz\right)$$

322 where β captures the overall scaling of transmission and N_t is the total host population
 323 size at time t . For the purposes of this illustration, we assume that there is no waning
 324 of immunity. The time course of infection in one exemplar clone, the AS clone, and
 325 associated model fits are shown in Figure 2A. The full set of 8 clones is shown in
 326 Figure S1. These clones have been characterized as falling along a virulence-
 327 transmission trade-off – the clones that result in the greatest anaemia also have the
 328 highest parasite loads, presumed to correlate with transmission (Metcalf *et al.* 2012).
 329

330 Such a pattern is an expected evolutionary outcome – both low and high virulence
331 pathogens might achieve equivalent fitness and coexist if the fitness cost resulting
332 from host mortality experienced by high virulence pathogens is offset by high rates of
333 transmission (Anderson & May 1982). However, the degree to which within-host
334 patterns suggestive of a virulence-transmission trade-off translate into the population
335 scale pattern that evolutionary predictions would suggest is unclear.

336 To evaluate outcomes at the population scale from this model, we first
337 combine the regression models fit to the dynamics of log infected RBCs (Figure 2B,
338 Figure S1, Table 1) with assumptions about how the burden of infected RBCs affects
339 survival and recovery probabilities (Figure 2C), and then numerically integrate the
340 resulting IPM using the ‘midpoint rule’ (Rees, Childs & Ellner 2014). With this, we
341 can project the population forwards and track densities of log infected RBCs (Figure
342 S2) as well as the process of infection.

343 Malaria has been held up as a powerful example of the virulence-transmission
344 trade-off (Mackinnon & Read 2004b), and the set of clones available in these data
345 illustrate this very clearly, with the clones that lead to the greatest anemia also having
346 the highest peaks of parasite density, and thus, by inference, transmission potential
347 (Figure 2D). However, these patterns describe individual host level outcomes. The
348 degree to which “transmission potential” translates to population level outcomes such
349 as incidence of infection is unclear (Alizon *et al.* 2009). Using our IPM framework,
350 we can evaluate this across the eight clones presented here, comparing the probability
351 that a susceptible individual will be infected at equilibrium, ϕ_t , with the depth of the
352 trough of anemia for each clone (Figure 2D). If the population scale outcomes
353 simply reflect within host outcomes, we would expect that the most virulent clones
354 (i.e., those associated with the greatest parasite density) are also the clones that pose
355 the highest risk to susceptible individuals – i.e., a positive relationship. In fact, we
356 find that the virulence-transmission pattern expected is considerably diluted with the
357 full population model – although virulent strains, for which the trough of RBCs is
358 particularly deep, tend to have high ϕ_t at equilibrium, the pattern across the clones
359 reverses the trade-off, and the least virulent clone (CW) achieves substantially more
360 transmission than within-host pattern predicts. In other words, processes occurring
361 across scales obscure the outcome we would expect from a virulence-transmission
362 trade-off at the scale of the host individual – and in fact, one might conclude that the

363 host level pattern is less an outcome of selection than a simple emergent property of
364 the process of infection in malaria – inevitably, gain of one infected RBC requires loss
365 of one uninfected RBC.

366 Intriguingly, these results also suggest that at the population level scale, the
367 AS clone deviates from the broad positive relationship seen across the other clones,
368 and has a much lower risk of onward transmission to susceptible individuals, ϕ_i . The
369 AS clone has an especially long history of propagation through serial passage, which
370 is expected to select for increased virulence (Mackinnon & Read 2004a) – this
371 adaptation might diminish performance when a population level perspective is taken,
372 as is suggested here (Figure 2D). However, the many components of the model for
373 which we did not introduce clone specific parameters (gametocyte production, and
374 particularly, recovery) might either diminish or accentuate this result. This is an
375 exciting area for future research.

376 There are a number of issues that should also be considered in evaluating the
377 patterns reported, and which are of more general importance in considering the utility
378 of IPMs for capturing within-host dynamics. First, the time-course available does not
379 entirely resolve the full infection for the range of clones (Figure S1) - in fact, many
380 clones experience secondary increases before the end of the time-course
381 (recrudescence), and few mice have recovered – without detailed parameterization of
382 this process, the IPM cannot capture it, and therefore may under or over estimate
383 population level outcomes as a result. This is likely to be a very general consideration
384 in both experimental and natural systems. Since the force of infection in the
385 population will depend on transmission across individuals at all stages of the
386 infection, the model will be sensitive to the exact choice of maximal days post-
387 infection modelled (J) as well as the parameterization of the recovery process.
388 Furthermore, choice of insufficiently large J , may result in heaping in the categories
389 corresponding to the last day post-infection modelled, or unintentional eviction from
390 the IPM (see Williams, Miller & Ellner (2012) for more discussion of this issue). On
391 the positive side, further sensitivity analysis (such as exploration of the consequences
392 of parameter perturbation (Caswell 2001), albeit keeping in mind the caveats outlined
393 above) with the IPM framework would allow evaluation of exactly how important
394 these last infection processes are, and which are the key parameters for which further

395 investment and investigation would be most beneficial. Sensitivity to survival, fertility
396 and transmission parameters could likewise be explored.

397

398 **Case study 2: Exploring dynamical consequences of individual variability in**
399 **immune parameters: maternal immunity to measles**

400 Women who have been exposed to measles during their lifetime and developed
401 antibodies to this parasite can transfer those antibodies to their offspring (Nicoara *et*
402 *al.* 1999). Following birth, these transferred antibodies continue to protect the child
403 from infection by measles. However, maternally transferred antibodies degrade over
404 time, and once their concentration has waned to negligible levels, offspring are once
405 again vulnerable to measles (Cáceres, Strebel & Sutter 2000). The exact magnitude of
406 the transferred antibodies affects the time until susceptibility, and can thus have
407 population level consequences. Furthermore, vaccinated mothers are known to
408 transfer lower levels of antibodies to their children, a phenomenon echoed by
409 heterogeneities in transfer of maternal antibodies observed from birds to mammals
410 (Boulinier & Staszewski 2008), and the dynamical consequences of this are still
411 unresolved.

412 We use data and models presented in (Waaaijenborg *et al.* 2013) to develop
413 regression models to capture the pattern of decline of maternal antibodies as a
414 function of current levels (obtained by simulating from the model they develop to
415 describe antibody concentration as a function of age), as well as initial densities and
416 threshold marking the transition to susceptibility (Figure 3A-C, Table 2). As above,
417 we nest this within an SIR framework but now including a 'V' category for
418 vaccinated individuals:

$$S(z', t + 1) = (1 - v)[A_0(z')B + A_{0v}(z')B_v] + s \int_L^U A(z', z)(1 - \phi(z, t))S(z, t)dz$$

$$I(t + 1) = s \int_L^U A(z', z)\phi(z, t)S(z, t)dz$$

$$R(t + 1) = sR(t) + sI(t)$$

419 $V(t + 1) = v[B + B_v] + sV(t)$

420

421 where $S(z, t)$ reflects the number of susceptible individuals with maternal antibody
422 concentration z , $I(t)$ is the number of infected individuals, $R(t)$ the number of

423 recovered (and completely immune) individuals and $V(t)$ is the number of vaccinated
424 individuals (also completely immune). We could also have chosen to model an
425 explicit maternally immune or ‘M’ compartment, but instead chose to consider
426 maternal antibodies as indicative of susceptibility status for simplicity. The time-step
427 here is taken as two weeks, which reflects the approximate generation time of measles
428 (Grenfell, Bjornstad & Finkenstädt 2002). The probability of vaccination in one two-
429 week time-step is captured by v ; s is the probability of survival (we ignore infection
430 related mortality for simplicity), f is fertility, likewise, and $\phi(z,t)$ is the probability of
431 infection of an individual with maternal antibody concentration z (further detailed
432 below). At birth, the distribution of maternal antibody concentrations in infants is
433 captured by the density function $A_0(z)$ for unvaccinated mothers, and $A_{0v}(z)$ for
434 vaccinated mothers; where B indicates the number of children born to unvaccinated
435 mothers and B_v children born to vaccinated mothers; subsequent decline of maternal
436 antibodies is captured by the kernel $A(z',z)$; the integration occurs between an upper
437 and lower limit of antibody concentrations U and L , and recovery is complete within
438 one two week period, so all infected individuals moved into the recovered stage at
439 $t+1$; see Table 2 for details of parameters and functional forms. The probability of
440 infection, $\phi(z,t)$ is defined by

441
442
$$\phi(z,t) = (1 - \exp(-\beta_t I(t)/N_t))p(z)$$

443
444 where β_t captures seasonally varying transmission, N_t is the total host population size
445 at time t , included as immunizing childhood infections generally scale in a frequency
446 dependent fashion (Grenfell, Bjornstad & Finkenstädt 2002), and $p(z)$ reflects the
447 probability of being susceptible, for an individual with antibody concentration z .

448 To illustrate the use of IPMs in this setting, we simulated two contrasting
449 situations – in both, vaccination was introduced, but in the first case, the observed
450 difference between the offspring of vaccinated and unvaccinated mothers was
451 implemented, and in the second, we assumed that this difference did not exist, i.e.,
452 $a_{0v}=a_{0s}$ (Table 2, Figure 3D). Intriguingly, if vaccinated mothers supply their children
453 with just as high a concentration of antibodies as unvaccinated mothers, this can
454 nevertheless actually result in a higher burden of cases. This illustrates the importance
455 of non-linear feedbacks that characterize infectious disease dynamics – in this

456 example, specifically, the effect of ‘honeymoons’ resulting from vaccination (McLean
457 & Anderson 1988). Classically, this occurs because introduction of vaccination
458 reduces transmission, thus leaving individual who are unvaccinated also unexposed to
459 natural infection, allowing accumulation of susceptible individuals, potentially
460 eventually resulting in a large outbreak. Here, the twist is that the absence of maternal
461 protection in vaccinated individuals prevents the longer build-ups of susceptible
462 individuals, by accelerating waning of immunity, and allowing earlier, and thus
463 smaller outbreaks. Removing this difference has the opposite effect – amplifying the
464 honeymoon effect. By extension, it can clearly be seen that individual differences
465 such as those described here linked to vaccination can have population level
466 dynamical consequences. Further evaluation of the effects of individual heterogeneity
467 as well as the trajectory of waning of immunity could be undertaken with the
468 framework described here.

469

470 **Discussion**

471 The overview we present here, in conjunction with the two case studies, suggest that
472 there is considerable potential for using IPMs to understand the consequences of
473 continuous traits for infectious disease dynamics, while also highlighting some of the
474 technical challenges. These include all the usual issues experienced in IPM
475 development (Williams, Miller & Ellner 2012), as well as some of the more subtle
476 issues in interpretation and model construction, such as issues of extrapolating the
477 regressions beyond the range of the data (Merow *et al.* 2014).

478 For any particularly study system, a further important consideration in
479 evaluating the value of an IPM approach is the quality and characteristics of the data
480 available. Longitudinal data that captures individual trajectories in the focal trait (such
481 as pathogen load or antibody titer), as well as variance across individuals are essential.
482 Data that captures the full time-course of the infection process will also be key, as
483 appropriately detailing the process of recovery (or not) will be essential for capturing
484 dynamics (see Case Study 1). In the absence of such data, inverse modelling
485 approaches where population scale data, such as relative abundance of individuals of
486 different sizes, or prevalence of the infection, are used to strengthen inference (e.g.,
487 Cropper & Anderson 2004) may provide some power, but parameter identifiability is
488 likely to be a major challenge. Broader data on the ecology and life history of the
489 species will also be important for robust prediction. For example, seasonal birth

490 pulses shape the ecology of many rodent species, and may have profound effects on
491 disease dynamics (Peel *et al.* 2014). It is straightforward to extend the models
492 described here to incorporate such ecological realism. A particularly interesting
493 dimension may be interaction between host ‘condition’ (often captured by some
494 measure of body mass) and parasite or immune dynamics. Host condition may be
495 influenced by disease burden and past environmental conditions. Since infection risk
496 may in turn depend on the condition of individual hosts (Koski & Scott 2001;
497 Beldomenico & Begon 2010), there is potential for feedbacks between the
498 transmission processes and host trait dynamics, leading to complex both ecological
499 and evolutionary dynamics (Boots *et al.* 2009; Hayward *et al.* 2014a).

500 Our focus in the two case studies presented has been on traits that reflect
501 dynamical heterogeneity (Vindenes & Langangen 2015), which various lines of
502 evidence suggest may be key to understanding ecological and evolutionary processes.
503 For example, analyses of reproductive timing in a monocarpic perennial herb have
504 shown that among-individual variation in growth trajectories influences the age-
505 distribution of reproductive timing, and that the costs and benefits of this variation are
506 influenced by (among other factors) temporal variation in the mean annual growth
507 rate (Childs *et al.* 2004; Rees *et al.* 2004). There has also been a recent expansion of
508 analyses of the consequences of static heterogeneity (Vindenes & Langangen 2015),
509 i.e., traits that vary across individuals, but that an individual will retain for its entire
510 life. Failure to include such static heterogeneity into models has been shown to result
511 in mis-estimation of both the long-term population growth rate, but also an array of
512 other key life history variables such as the mean age of mothers (Vindenes &
513 Langangen 2015). Considering such features is likely to be of particular importance in
514 models capturing infectious diseases, as there is considerable evidence for strong
515 genetic or early environment signatures on responses to infection (Hill 1998).

516 The default tool for modelling infectious disease dynamics in structured
517 populations has long been Partial Differential Equations (Anderson & May 1991).
518 The two case studies presented here suggest that IPMs might provide a tractable, data-
519 driven alternative. However, the degree to which IPMs are applicable for
520 epidemiological systems will depend very much on the scale of data available – if
521 data only exists at time-steps that prove too coarse for regression-based tools to
522 capture the detail of within host dynamics, then IPMs are unlikely to be the best
523 modelling approach. A major challenge to deploying IPMs for questions in the

524 ecology and evolution of infectious disease may therefore be that the level of fine-
525 scale detail explored here is likely to be only rarely available, especially in field
526 systems. On the other hand, IPMs might offer a framework for more theoretical
527 investigations – for example, allowing investigation of specific functional forms and
528 their effects on disease dynamics, providing a framework for generating hypotheses.

529 An array of powerful tools have been developed for matrix population models
530 (Caswell 2001; Klepac & Caswell 2011) and extended for IPMs (e.g., Ellner & Rees,
531 2007), opening the way to evaluating the impact of an array of important features such
532 as stochasticity on disease dynamics in an IPM framework. There are also a number
533 of open directions for interesting technical developments – for example, building on
534 innovations linking age and stage with infectious disease dynamics in a matrix
535 framework (Klepac & Caswell 2011), it should be possible to derive descriptors of the
536 expected number of secondary infections depending on the underlying initial parasite
537 burden (e.g., $R_0(z)$). This would provide interesting ways to quantify the impact of
538 individuals with underlying focal trait value x on the dynamics of infection, a
539 statistically rooted way of tackling the role of super-spreaders (Lloyd-Smith *et al.*
540 2005).

541 The two case studies we provide both use phenomenological models to capture
542 the complexity of feedback driven dynamics of the process of infection, thereby
543 providing an abstraction of the true dynamics (feedbacks between immunity and
544 parasitaemia, for instance). For maternal antibodies, where the process is unlikely to
545 respond to perturbations such as infection (Cáceres, Strebel & Sutter 2000), this
546 strategy is likely to be relatively robust. In the case of murine malaria, blood stage
547 dynamics essentially reflect an SIR process themselves (Mideo *et al.* 2008; Metcalf *et*
548 *al.* 2011; Metcalf *et al.* 2012), and careful interpretation of model predictions given
549 the potential for unpredictable feedbacks is essential. While the phenomenological
550 approach described is likely to be powerful for taking a comparative perspective, as
551 illustrated above using clones with varying levels of virulence (populations, or
552 environments could be similarly deployed), it precludes more dynamical
553 investigations of the outcome of perturbations. For example, with the
554 phenomenological models we develop, exploring the impact of increasing the rate of
555 growth of the infected RBC population is impossible, as there is nothing in the model
556 to describe how increased parasite load will increase immune activity. However, in
557 principle, we could easily embed a further SIR within the host level SIR to capture the

558 details of within host dynamics, aligning for example, infected cell survival with host
559 immune activity, as our response variable. This would enable fine scale analysis of the
560 evolutionary consequences of changes in within host traits, such as allocation towards
561 sexual reproduction and its fluctuations through time (Mideo & Day 2009), or
562 synchrony in bursting of red blood cells (Mideo *et al.* 2013; Greischar, Read &
563 Bjørnstad 2014).

564 To conclude, using IPMs to bring continuous traits to infectious disease
565 models has the potential to provide a powerful new approach to tackling an array of
566 important questions in animal ecology and evolution. As illustrated here with the
567 rodent malaria example, leveraging a breadth of data to develop phenomenological
568 models capturing interactions between underlying mechanistic processes can yield
569 comparative insights into cross-scale dynamics. For models, or model components,
570 where the mechanisms are more directly reflected, perturbation analyses will also
571 allow for exciting ecological and evolutionary developments. For example,
572 explorations of the evolutionary dynamics of pathogen load, using approaches
573 analogous to those used to explore timing of flowering of monocarpic plants (Metcalf
574 *et al.* 2008) could generate new, and importantly, empirically grounded insights into
575 virulence-transmission trade-offs. The density and/or frequency dependence of
576 infectious disease dynamics could result in hard to predict evolutionary feedbacks
577 linked to this trait, which might be captured using adaptive dynamics approaches
578 (Dieckmann 1997). At a more ecological scale, the feedbacks inherent to infectious
579 disease dynamics can lead to non-intuitive outcomes, making models key to
580 generating expectations; however, this also leads to highly sensitive dynamics, with
581 complex transients, which can make empirically rooted models essential to predicting
582 short-term outcomes of underlying continuous traits. Overall, this is a promising area
583 of research, and one in which we expect an array of technical developments in coming
584 years.

585

586 **Acknowledgements:** This work emerged from a BES funded conference entitled
587 ‘Demography beyond the Population’, and was funded by a NERC fellowship
588 (NE/I022027/1 to D.Z.C.), the RAPIDD program of the Science & Technology
589 Directorate, Department of Homeland Security and the Fogarty International Center,
590 National Institutes of Health (C.J.E.M., A.L.G); and was inspired partly by
591 discussions arising from an NSF-funded Research Coordination Network on

592 Infectious Disease Evolution across Scales and during the development of a NSF-
593 funded postdoctoral fellowship (Award Number: 1523757 to M.M.B).

594

595 **Data accessibility**

596 Malaria data is available from the Dryad Digital Repository

597 <http://dx.doi.org/10.5061/dryad.07mc1> (Metcalf et al. 2016).

598

599 **References**

600 Alizon, S., Hurford, A., Mideo, N. & Van Baalen, M. (2009) Virulence evolution and
601 the trade-off hypothesis: history, current state of affairs and the future.

602 *Journal of Evolutionary Biology*, **22**, 245-259.

603 Anderson, R.M. & May, R.M. (1982) Coevolution of hosts and parasites. .

604 *Parasitology*, **85**, 411-426.

605 Anderson, R.M. & May, R.M. (1991) *Infectious diseases of humans*. Oxford

606 University Press, Oxford, OX2 6PD.

607 Antia, R., Ganusov, V.V. & Ahmed, R. (2005) The roles of models in understanding

608 CD8+ T-cell memory. *Nature Reviews Immunology*, **5**, 101-111.

609 Antia, R. & Lipstich, M. (1997) Mathematical models of parasite responses to host

610 immune defenses. *Parasitology*, **115**, S115-S167.

611 Beldomenico, P.M. & Begon, M. (2010) Disease spread, susceptibility and

612 infection intensity: vicious circles? *Trends in Ecology & Evolution*, **25**, 21-
613 27.

614 Bjørnstad, O.N., Finkenstadt, B. & Grenfell, B.T. (2002) Endemic and epidemic

615 dynamics of measles: Estimating epidemiological scaling with a time

616 series SIR model. *Ecological Monographs*, **72**, 169-184.

617 Bonhoeffer, S., Fraser, C., Leventhal, G.E. & Swanstrom, R. (2015) High

618 Heritability Is Compatible with the Broad Distribution of Set Point Viral

619 Load in HIV Carriers. *PLoS Pathogens*, **11**, e1004634-e1004634.

620 Boots, M., Best, A., Miller, M.R. & White, A. (2009) The role of ecological feedbacks

621 in the evolution of host defence: what does theory tell us? *Philosophical*

622 *Transactions of the Royal Society B: Biological Sciences*, **364**, 27-36.

623 Borchers, S., Ogonek, J., Varanasi, P.R., Tischer, S., Bremm, M., Eiz-Vesper, B.,

624 Koehl, U. & Weissinger, E.M. (2014) Multimer monitoring of CMV-specific

625 T cells in research and in clinical applications. *Diagnostic microbiology and*
626 *infectious disease*, **78**, 201-212.

627 Boulinier, T. & Staszewski, V. (2008) Maternal transfer of antibodies: raising
628 immuno-ecology issues. *Trends in Ecology & Evolution*, **23**, 282-288.

629 Brook, C.E. & Dobson, A.P. (2015) Bats as 'special' reservoirs for emerging
630 zoonotic pathogens. *Trends in Microbiology*.

631 Cáceres, V.M., Strebel, P.M. & Sutter, R.W. (2000) Factors determining prevalence
632 of maternal antibody to measles virus throughout infancy: a review.
633 *Clinical infectious diseases*, **31**, 110-119.

634 Caswell, H. (2001) *Matrix population models*. Wiley Online Library.

635 Childs, D., Coulson, T., Pemberton, J., Clutton-Brock, T. & Rees, M. (2011)
636 Predicting trait values and measuring selection in complex life histories:
637 reproductive allocation decisions in Soay sheep. *Ecology Letters*, **14**, 985-
638 992.

639 Childs, D.Z., Rees, M., Rose, K.E., Grubb, P.J. & Ellner, S.P. (2003) Evolution of
640 complex flowering strategies: an age- and size-structured integral
641 projection model. *Proceedings of the Royal Society of London B: Biological*
642 *Sciences*, **270**, 1829-1838.

643 Childs, D.Z., Rees, M., Rose, K.E., Grubb, P.J. & Ellner, S.P. (2004) Evolution of size-
644 dependent flowering in a variable environment: construction and analysis
645 of a stochastic integral projection model. *Proceedings of the Royal Society*
646 *of London B: Biological Sciences*, **271**, 425-434.

647 Chung, Y.A., Miller, T.E. & Rudgers, J.A. (2015) Fungal symbionts maintain a rare
648 plant population but demographic advantage drives the dominance of a
649 common host. *Journal of Ecology*.

650 Cropper, W.P. & Anderson, P.J. (2004) Population dynamics of a tropical palm:
651 use of a genetic algorithm for inverse parameter estimation. *Ecological*
652 *modelling*, **177**, 119-127.

653 Dieckmann, U. (1997) Can adaptive dynamics invade? *Trends in Ecology &*
654 *Evolution*, **12**, 128-131.

655 Easterling, M.R., Ellner, S.P. & Dixon, P.M. (2000) Size-specific sensitivity:
656 applying a new structured population model. *Ecology*, **81**, 694-708.

- 657 Ellner, S.P., Jones, E., Mydlarz, L.D. & Harvell, C.D. (2007) Within-host disease
658 ecology in the sea fan *Gorgonia ventalina*: modeling the spatial
659 immunodynamics of a coral-pathogen interaction. *American Naturalist*,
660 **170**, E143-E161.
- 661 Ellner, S.P. & Rees, M. (2006) Integral projection models for species with complex
662 demography. *The American Naturalist*, **167**, 410-428.
- 663 Ellner, S.P. & Rees, M. (2007) Stochastic stable population growth in integral
664 projection models: theory and application. *Journal of mathematical*
665 *biology*, **54**, 227-256.
- 666 Ford, K.R., Ness, J.H., Bronstein, J.L. & Morris, W.F. (2015) The demographic
667 consequences of mutualism: ants increase host-plant fruit production but
668 not population growth. *Oecologia*, 1-12.
- 669 Gilchrist, M.A., Coombs, D. & Perelson, A.S. (2004) Optimizing within-host viral
670 fitness: infected cell lifespan and virion production rate *Journal of*
671 *Theoretical Biology*, **229**, 281-288.
- 672 Gog, J.R., Pellis, L., Wood, J.L., McLean, A.R., Arinaminpathy, N. & Lloyd-Smith, J.O.
673 (2014) Seven challenges in modeling pathogen dynamics within-host and
674 across scales. *Epidemics*.
- 675 Graham, A.L. (2008) Ecological rules governing helminth-microparasite co-
676 infection. *Proc Natl Acad Sci U S A*, **105**, 566-570.
- 677 Graham, A.L., Allen, J.E. & Read, A.F. (2005) Evolutionary causes and
678 consequences of immunopathology. *Annual Review of Ecology, Evolution,*
679 *and Systematics*, 373-397.
- 680 Graham, A.L., Cattadori, I.M., Lloyd-Smith, J.O., Ferrari, M.J. & Bjørnstad, O.N.
681 (2007) Transmission consequences of coinfection: cytokines writ large?
682 *Trends in Parasitology*, **23**, 284-291.
- 683 Graham, A.L., Hayward, A.D., Watt, K.A., Pilkington, J.G., Pemberton, J.M. & Nussey,
684 D.H. (2010) Fitness correlates of heritable variation in antibody
685 responsiveness in a wild mammal. *Science*, **330**, 662-665.
- 686 Greischar, M.A., Read, A.F. & Bjørnstad, O.N. (2014) Synchrony in malaria
687 infections: how intensifying within-host competition can be adaptive. *The*
688 *American Naturalist*, **183**, E36-E49.

- 689 Grenfell, B.T., Bjornstad, O.N. & Finkenstädt, B.F. (2002) Dynamics of measles
690 epidemics: scaling noise, determinism, and predictability with the TSIR
691 model. *Ecological Monographs*, **72**, 185-202.
- 692 Haydon, D.T., Matthews, L., Timms, R. & Colegrave, N. (2003) Top-down or
693 bottom-up regulation of intra-host blood-stage malaria: do malaria
694 parasites most resemble the dynamics of prey or predator? *Proceedings of*
695 *the Royal Society of London - Series B*, **270**, 289-298.
- 696 Hayward, A.D., Garnier, R., Watt, K.A., Pilkington, J.G., Grenfell, B.T., Matthews, J.B.,
697 Pemberton, J.M., Nussey, D.H. & Graham, A.L. (2014a) Heritable,
698 Heterogeneous, and Costly Resistance of Sheep against Nematodes and
699 Potential Feedbacks to Epidemiological Dynamics*. *The American*
700 *Naturalist*, **184**, S58-S76.
- 701 Hayward, A.D., Nussey, D.H., Wilson, A.J., Berenos, C., Pilkington, J.G., Watt, K.A.,
702 Pemberton, J.M. & Graham, A.L. (2014b) Natural selection on individual
703 variation in tolerance of gastrointestinal nematode infection. *PloS Biology*,
704 **12**, e1001917.
- 705 Heffernan, J. & Keeling, M.J. (2009) Implications of vaccination and waning
706 immunity. *Proceedings of the Royal Society of London B: Biological*
707 *Sciences*, rspb. 2009.0057.
- 708 Hill, A.V. (1998) The immunogenetics of human infectious diseases. *Annual*
709 *review of immunology*, **16**, 593-617.
- 710 Klepac, P. & Caswell, H. (2011) The stage-structured epidemic: linking disease
711 and demography with a multi-state matrix approach model. *Theoretical*
712 *Ecology*, **4**, 301-319.
- 713 Koski, K.G. & Scott, M.E. (2001) Gastrointestinal nematodes, nutrition and
714 immunity: breaking the negative spiral. *Annual review of nutrition*, **21**,
715 297-321.
- 716 Kouyos, R.D., Metcalf, C.J.E., Birger, R., Klein, E.Y., zur Wiesch, P.A., Ankomah, P.,
717 Arinaminpathy, N., Bogich, T.L., Bonhoeffer, S. & Brower, C. (2014) The
718 path of least resistance: aggressive or moderate treatment? *Proceedings of*
719 *the Royal Society B: Biological Sciences*, **281**, 20140566.

720 Lloyd-Smith, J.O., Schreiber, S.J., Kopp, P.E. & Getz, W.M. (2005) Superspreading
721 and the effect of individual variation on disease emergence. *Nature*, **438**,
722 355-359.

723 Long, G.H., Chan, B.H., Allen, J.E., Read, A.F. & Graham, A.L. (2008a) Blockade of
724 TNF receptor 1 reduces disease severity but increases parasite
725 transmission during *Plasmodium chabaudi chabaudi* infection.
726 *International Journal for Parasitology*, **38**, 1073-1081.

727 Long, G.H., Chan, B.H.K., Allen, J.E., Read, A.F. & Graham, A.L. (2008b)
728 Experimental manipulation of immune-mediated disease and its fitness
729 costs for rodent malaria parasites. *BMC Evolutionary Biology*, **8**, 128.

730 Mackinnon, M.J. & Read, A.F. (1999) Genetic relationships between parasite
731 virulence and transmission in the rodent malaria *Plasmodium chabaudi*.
732 *Evolution*, **53**, 689-703.

733 Mackinnon, M.J. & Read, A.F. (2004a) Immunity promotes virulence evolution in
734 a malaria model. *PloS Biology*, **2**, e230.

735 Mackinnon, M.J. & Read, A.F. (2004b) Virulence in malaria: an evolutionary
736 viewpoint. *Phil Trans R Soc Lond B*, **359**, 965-986.

737 McLean, A. & Anderson, R. (1988) Measles in developing countries. Part II. The
738 predicted impact of mass vaccination. *Epidemiology and infection*, **100**,
739 419-442.

740 Merow, C., Dahlgren, J.P., Metcalf, C.J.E., Childs, D.Z., Evans, M.E., Jongejans, E.,
741 Record, S., Rees, M., Salguero-Gómez, R. & McMahon, S.M. (2014)
742 Advancing population ecology with integral projection models: a practical
743 guide. *Methods in Ecology and Evolution*, **5**, 99-110.

744 Metcalf, C., Birger, R., Funk, S., Kouyos, R., Lloyd-Smith, J. & Jansen, V. (2014) Five
745 challenges in evolution and infectious diseases. *Epidemics*.

746 Metcalf, C., Long, G., Mideo, N., Forester, J., Bjørnstad, O. & Graham, A. (2012)
747 Revealing mechanisms underlying variation in malaria virulence: effective
748 propagation and host control of uninfected red blood cell supply. *Journal*
749 *of the Royal Society Interface*, **9**, 2804-2813.

750 Metcalf, C., Rose, K., Childs, D., Sheppard, A., Grubb, P. & Rees, M. (2008)
751 Evolution of flowering decisions in a stochastic, density-dependent

752 environment. *Proceedings of the National Academy of Sciences*, **105**,
753 10466-10470.

754 Metcalf, C.J.E., Graham, A.L., Huijben, S., Barclay, V.C., Long, G.H., Grenfell, B.T.,
755 Read, A.F. & Bjornstad, O.N. (2011) Partitioning Regulatory Mechanisms
756 of Within-Host Malaria Dynamics Using the Effective Propagation
757 Number. *Science*, **333**, 984-988.

758 Metcalf, C.J.E., McMahon, S.M., Salguero-Gómez, R. & Jongejans, E. (2013)
759 IPMPack: an R package for integral projection models. *Methods in Ecology
760 and Evolution*, **4**, 195-200.

761 Metcalf, C.J.E., Graham, A.L., Martinez-Bakker, M. & Childs, D.Z. (2016) Data from:
762 Opportunities and challenges of Integral Projection Models for modelling
763 host-parasite dynamics. *Dryad Digital Repository*
764 <http://dx.doi.org/10.5061/dryad.07mc1>

765 Mideo, N., Barclay, V.C., Chan, B.H.K., Savill, N.J., Read, A.F. & Day, T. (2008)
766 Understanding and predicting strain-specific patterns of pathogenesis in
767 the rodent malaria *Plasmodium chabaudi*. *American Naturalist*, **172**, E214-
768 E238.

769 Mideo, N. & Day, T. (2009) On the evolution of reproductive restraint in malaria.
770 *Proceedings of the Royal Society of London - Series B*, **275**, 1217-1224.

771 Mideo, N., Reece, S.E., Smith, A.L. & Metcalf, C.J.E. (2013) The Cinderella
772 syndrome: why do malaria-infected cells burst at midnight? *Trends in
773 Parasitology*, **29**, 10-16.

774 Molineaux, L. & Dietz, K. (1999) Review of intra-host models of malaria.
775 *Parassitologia*, **41**, 221-231.

776 Nicoara, C., Zach, K., Trachsel, D., Germann, D. & Matter, L. (1999) Decay of
777 passively acquired maternal antibodies against measles, mumps and
778 rubella viruses. *Clinical and Diagnostic Laboratory Immunology*, **6**, 868-
779 871.

780 Nussey, D.H., Watt, K.A., Clark, A., Pilkington, J.G., Pemberton, J.M., Graham, A.L. &
781 McNeilly, T.N. (2014) Multivariate immune defences and fitness in the
782 wild: complex but ecologically important associations among plasma
783 antibodies, health and survival. *Proceedings of the Royal Society B:
784 Biological Sciences*, **281**, 20132931.

785 Ozgul, A., Childs, D.Z., Oli, M.K., Armitage, K.B., Blumstein, D.T., Olson, L.E.,
786 Tuljapurkar, S. & Coulson, T. (2010) Coupled dynamics of body mass and
787 population growth in response to environmental change. *Nature*, **466**,
788 482-485.

789 Peel, A.J., Pulliam, J., Luis, A., Plowright, R., O'Shea, T., Hayman, D., Wood, J., Webb,
790 C. & Restif, O. (2014) The effect of seasonal birth pulses on pathogen
791 persistence in wild mammal populations. *Proceedings of the Royal Society*
792 *B: Biological Sciences*, **281**, 20132962.

793 Perelson, A.S. (2002) Modeling viral and immune system dynamics. *Nature*
794 *Reviews Immunology*, **2**, 28-36.

795 Rees, M., Childs, D.Z. & Ellner, S.P. (2014) Building integral projection models: a
796 user's guide. *Journal of Animal Ecology*, **83**, 528-545.

797 Rees, M., Childs, D.Z., Rose, K.E. & Grubb, P.J. (2004) Evolution of size-dependent
798 flowering in a variable environment: partitioning the effects of fluctuating
799 selection. *Proceedings of the Royal Society of London B: Biological Sciences*,
800 **271**, 471-475.

801 Saenz, R.A., Quinlivan, M., Elton, D., MacRae, S., Blunden, A.S., Mumford, J.A., Daly,
802 J.M., Digard, P., Cullinane, A., Grenfell, B.T., McCauley, J.W., Wood, J.L.N. &
803 Gog, J.R. (2010) Dynamics of influenza virus infection and pathology.
804 *Journal of Virology*, **84**, 3974-3983.

805 Vindenes, Y. & Langangen, Ø. (2015) Individual heterogeneity in life histories and
806 eco-evolutionary dynamics. *Ecology Letters*, **18**, 417-432.

807 Waaijenborg, S., Hahné, S.J., Mollema, L., Smits, G.P., Berbers, G.A., van der Klis,
808 F.R., de Melker, H.E. & Wallinga, J. (2013) Waning of maternal antibodies
809 against measles, mumps, rubella, and varicella in communities with
810 contrasting vaccination coverage. *Journal of Infectious Diseases*, **208**, 10-
811 16.

812 Williams, J.L., Miller, T.E. & Ellner, S.P. (2012) Avoiding unintentional eviction
813 from integral projection models. *Ecology*, **93**, 2008-2014.

814
815
816
817

818

819

820 **Table 1:** Parameters and functional forms for IPMs relating to murine malaria;
 821 indicating parameters for the AD clone, shown in Figure 2A. The full array of
 822 parameters across clones is shown in supplement S1. For the numerical integration,
 823 we set the upper limit of integration $U=12$, the lower limit $L=3$, and the number of
 824 days post-infection tracked to be $J=15$.

825

Description	Functional form	Parameters	Details of parameterization
Dynamics of log infected RBCs, $G_j(z', z)$	$z_t = a_g + b_g z_{t-1} + c_g j + d_g j^2 + \varepsilon$	$a_g=4.83, b_g=-0.11, c_g=0.51, d_g=-0.0003, \varepsilon = N(0, \sigma=0.43)$	Fitted to data
Starting density of z on infection, $G_0(z')$	$z_0 = a_0 + \omega$	$a_0 = 6.75; \omega = 0.37$	Fitted to data
Survival of infected individuals	$\text{logit}(s_z(x)) = m_0 + m_s x$	$m_0 = 30, m_s = -3$	Specified to result in mortality for mice with $z > x$, based on previous analyses
Recovery of infected individuals	$\text{logit}(r_j(x)) = r_0 + r_s x$	$r_0 = 26, r_s = -4 \text{ for } j < J$	Specified to result in recovery if z falls below 7; and for $j=J$, in the absence of further information, we set $r_j=1$
Survival of uninfected individuals	s	0.997	Based on an average mouse lifespan of 12 months
Fertility	f	0.13	Based on average

			mouse fertility of 5 litters of 10 mice per year
Transmission	β	5	Assuming approximately 5 new infections per infected individual.

826
827
828
829
830
831

Table 2: Parameters and functional forms for IPMs relating to maternal antibodies of measles. For the numerical integration, we set the lower limit of integration $L=-10$, and the upper limit $U=4$, based on data from (Waijenborg *et al.* 2013)

Description	Functional form	Parameters	Details of parameterization
Dynamics of waning of log maternal antibody concentration, z , $A(z',z)$	$m_t = a_g + b_g m_{t-1} + c_g m_{t-1}^2 + \varepsilon$	$a_g = -1.52$, $b_g = 0.94$, $c_g = 0.07$ $\varepsilon = N(0, \sigma = 1.28)$	Fitted to a simulation based on data described in Figure 1 of (Waijenborg <i>et al.</i> 2013); and parameters provided in the Supplement
Starting density of z for children born to infected mothers, $A_0(z')$	$z_{0s} = a_{0s} + \omega$	$a_{0s} = 1.74$; $\omega_s = 1.11$	Obtained from (Waijenborg <i>et al.</i> 2013)
Starting density of z for children born to vaccinated mothers, $A_{0v}(z')$	$z_{0v} = a_{0v} + \omega$	$a_{0v} = 0.48$; $\omega_s = 1.11$	Obtained from (Waijenborg <i>et al.</i> 2013)

Probability of being susceptible as a function of log maternal antibody concentration	$\text{logit}(s_s(z)) = s_0 + s_1 z$	$s_0 = 1.60; s_1 = -1$	Based on a cutoff titer of 1.60 for susceptibility (Waaijenborg <i>et al.</i> 2013)
Survival of uninfected individuals	s	0.99	Reflecting high biweekly survival
Total offspring each biweek	B	500	Reflecting a high fertility context
Transmission	β	18	Based on average R_0 for measles
Seasonal forcing function (t indexes biweek in the simulation)	$(1 + \alpha \cos(2\pi(t/24)))$	$\alpha = 0.5$	Based on observed patterns for measles

832

833

834 **Figure 1: Hypothetical example of the workflow for construction of an infectious**

835 **disease IPM.** A) Define the life-cycle (here a classic SIR, or Susceptible-Infected-

836 Recovered framework) and identify the continuous feature of within-host dynamics

837 that is the focal variable; here taken as viral load, and denoted by z ; B) Frame the

838 observed dynamics of z (here shown as a function of days post-infection on the x

839 axis), to allow an appropriate regression model to be fitted. Here, the data is re-plotted

840 to relate z one day in the future to the current value of z (grey points), which is well

841 described by a linear regression (red line); the density of z on the first day of infection

842 is also required to construct the IPM, and can be simply obtained by fitting a mean

843 and variance to the distribution of z observed on day 1; C) Use regression modelling

844 to describe the relationship between z and key host level outcomes, here taken to be

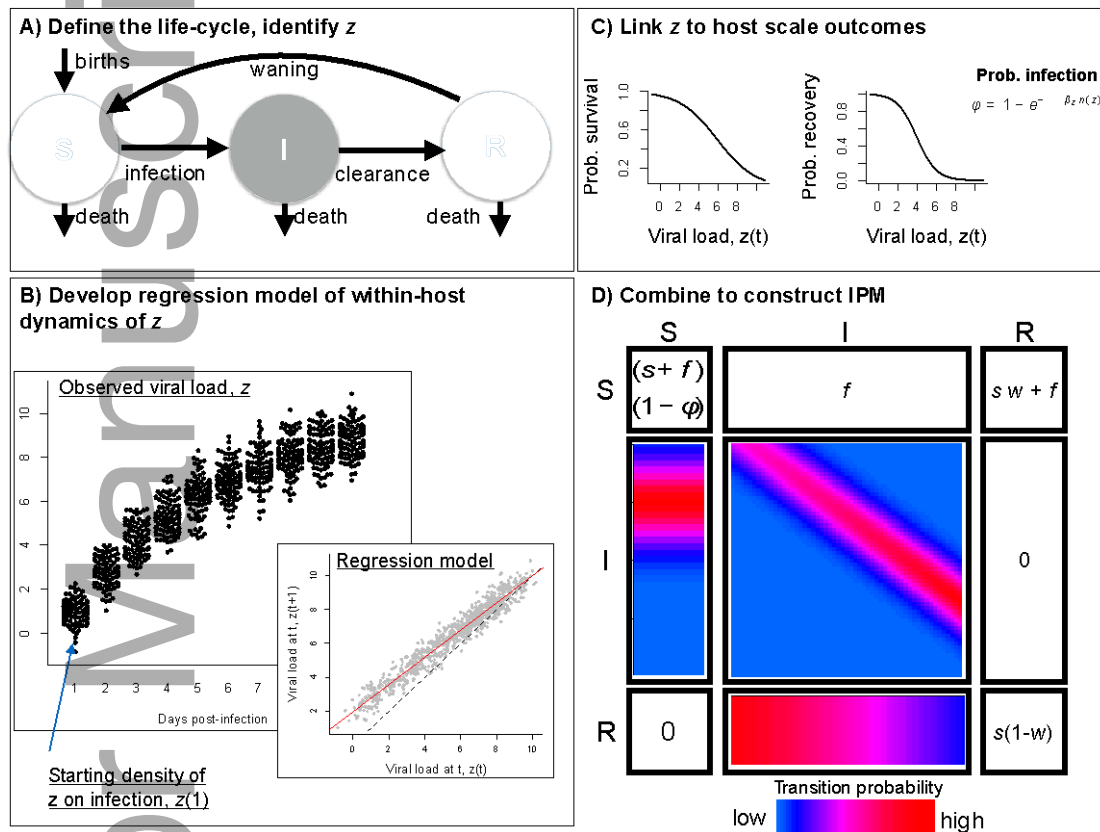
845 recovery and survival, and probability that a susceptible individual becomes infected,

846 ϕ . The latter depends on the relationship between viral load z and transmission, β_z as

847 well as $I(z)$, the number of individuals with viral load z . Other relationships are, of

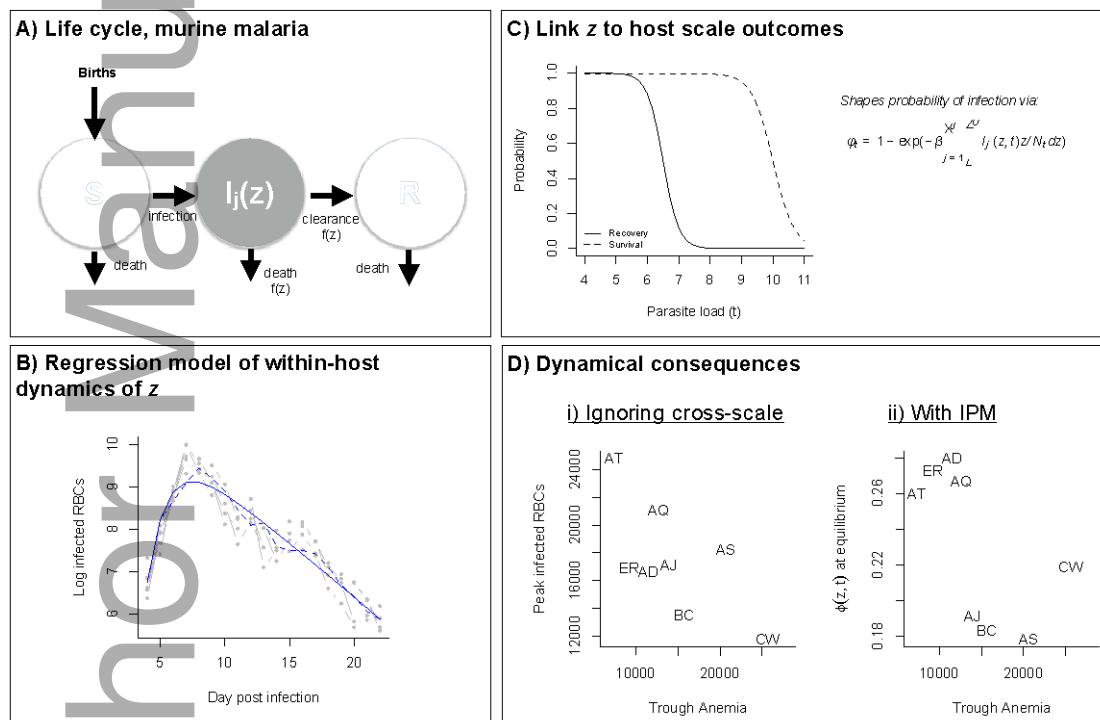
848 course, possible (e.g., with fertility) but are not illustrated here. D) Construct the

849 associated IPM model, where the transition from susceptibility to infection depends
 850 on the density of viral load across the population, and is associated with a starting
 851 density of viral load, z ; viral load evolves according to a linear regression over the
 852 course of the infection, and there is a probability of survival and recovery during
 853 infection associated with viral load. Other variables include survival of uninfected
 854 individuals, s , fertility, f , and the probability of waning of immunity, w .
 855



856
 857
 858
 859 **Figure 2: Constructing a model of murine malaria (following Figure 1).** A) The
 860 **life cycle**, with choice of parasite density as z , a variable which shapes both the rate of
 861 recovery and survival ($f(z)$ indicates a dependence on z); the Susceptible (S), Infected
 862 (I) and Recovered (R) classes all contribute to births, not shown for clarity. B)
 863 **Within-host dynamics** showing the time series of parasite density in the blood phase
 864 of malaria for five mice infected with the AD clone (grey points) and fitted linear
 865 regression predicted log infected RBCs as a function of current burden and time-step
 866 either one time-step ahead (dashed line) or over the full time course (solid line);
 867 parameters are provided in Table 1. Similar patterns are obtained for the 7 other

868 clones (Figure S1). C) **Host scale dynamics** including assumed patterns of recovery
 869 and survival as a function of the log infected RBC burden required to construct an
 870 IPM (see Table 1), and equation defining the probability of infection. D) **Comparison**
 871 **of broad inference** i) when ignoring cross scale-dynamics, the maximal infected
 872 RBCs observed over the time-course of infection across clones (y axis) is negatively
 873 associated with the depth of the trough of RBCs (x axis), an indicator of anemia, a
 874 relationship attributed to a virulence transmission trade-off (Metcalf *et al.* 2012); ii)
 875 Using an IPM to capture cross-scale dynamics indicates that the probability of
 876 infection of susceptible individuals at equilibrium estimated from the full IPM (y axis)
 877 shows no clear relationship with the trough of RBCs (x axis), suggesting that the
 878 cross-scale dynamics (incorporation of survival and recovery) dilute this effect.
 879

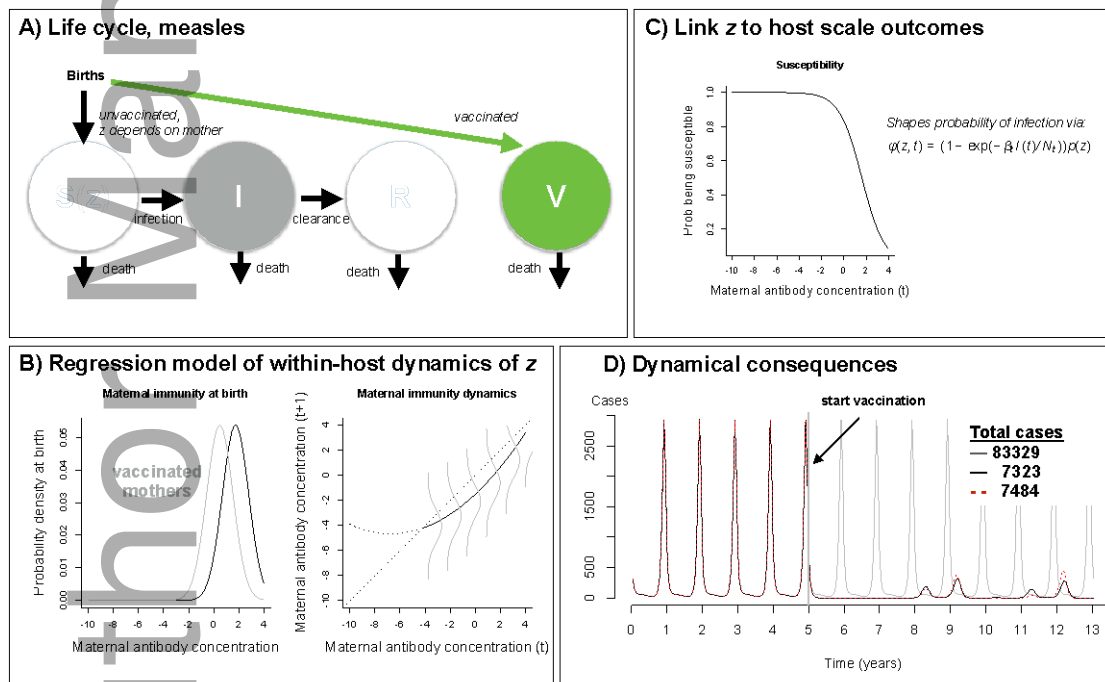


880

881

882 **Figure 3: Dynamical consequences of effects of vaccination on maternal**
 883 **antibodies (following Figure 1). A) The life cycle**, with choice of maternal
 884 antibodies as z , a variable which shapes the loss of susceptibility and thus infection
 885 ($f(z)$ indicates a dependence on z); the Susceptible (S), Infected (I) and Recovered (R)
 886 and Vaccinated (V) classes all contribute to births, and the level of z is defined by the
 887 identity of the mother, see text for details. B) **Within-host dynamics** showing the
 888 distribution of maternal antibodies at birth for unvaccinated (black) and vaccinated

889 (grey) mothers, and their subsequent decline; where the distribution around this
 890 decline obtained via a regression model (grey lines); C) **Host scale dynamics**
 891 including the probability of become susceptible as a function of maternal antibodies;
 892 see Table 2 for parameters and their sources. D) Simulations from the IPM model
 893 showing cases obtained under a simulation with no vaccination (grey line) and cases
 894 obtained under 85% vaccination when mothers do (black line) or do not (red dashed
 895 line) differ in their maternal immunity; indicating the counter-intuitive outcome that
 896 increased protection of offspring can actually result in more cases via non-linear
 897 effects. The legend indicates total cases after the start of vaccination in each of the
 898 three scenarios – both vaccination scenarios reduce the number of cases, but counter-
 899 intuitively, if vaccinated mothers transfer antibody concentrations as high as naturally
 900 infected mothers, the total number of cases may be higher as a result of transient
 901 dynamics.
 902



903